RESEARCH ARTICLE
Published: 18 August 2026

Volume 13 | Issue 2 | 451-462

OPEN ACCESS

Journal of Daylighting

Journal homepage: www.solarlits.com/jd

Self-Cleaning Effect in Coating Mortar Promoted by the Addition of Zinc Oxide

Eduarda Rafaella Novello,[1] Kim Lisbôa Daudt Maus,[1,] Eduardo Gomes,[1] Leticia Lange,[1] Ramon Mendonça Teles,[1] Alexandre Silva de Vargas,[2] Daiana Cristina Metz Arnold [1]*

[1] *Centro de Construções Sustentáveis, Universidade Feevale, Novo Hamburgo, Rio Grande do Sul, 93525-075, Brasil*

[2] *Departamento de Estruturas e Engenharia Civil, Universidade Federal de Santa Maria, Santa Maria, Rio Grande do Sul, 97105-900, Brasil*

ABSTRACT

The deterioration of building facades caused by both chemical agents and atmospheric pollutants has intensified considerably in recent years, leading not only to staining but also compromising the durability and aesthetics of coating mortars. The incorporation of photocatalysts into cementitious materials has emerged as a promising strategy to mitigate these effects due to their ability to decompose pollutants and microorganisms under ultraviolet (UV) radiation. This study aimed to evaluate the effect of incorporating 0, 1, 2, and 3% zinc oxide (ZnO) on the chemical, mechanical, and self-cleaning properties of white-cement coating mortars. Chemical characterization of ZnO, fresh and hardened state tests of the mortars, and self-cleaning performance evaluations were conducted through ultraviolet exposure in a UV light booth, assessing the degradation of methylene blue staining. The ZnO presented a hexagonal wurtzite structure and a specific surface area 26.44% higher than that of the reference mortar. The incorporation of 1% ZnO increased compressive strength by 12.90%, while flexural strength increased up to 40.90% with 3% ZnO, compared to the reference composition. Capillarity was reduced by up to 92.00% relative to the 0% ZnO composition. The self-cleaning performance was confirmed through colorimetric analysis and ΔE values, which indicated perceptible color changes in all samples, with the highest efficiency observed for compositions containing 2% and 3% ZnO, promoting greater degradation of stains. Overall, the results highlight the potential of ZnO to enhance both the mechanical performance and self-cleaning capability of mortars, contributing to the mitigation of staining and the preservation of durability and aesthetics over time.

Keywords: self-cleaning mortar; zinc oxide; photocatalysis; methylene blue

1. INTRODUCTION

Facades of buildings undergo degradation due to factors such as biological agents, atmospheric pollution and climatic conditions, whose intensity varies according to the environment in which the building is located. These elements reduce service life and performance, increasing maintenance needs [1]. Studies have identified that the main pathological manifestation found in mortar coatings is staining caused by the deposition of dirt from atmospheric particles and moisture.

This affects aesthetics, durability and habitability, increasing the recurrence of corrective maintenance [1-3]. In addition to the deterioration agents mentioned above, these pathological manifestations are also associated with facade orientation, solar incidence, mechanical corrosion, chemical attack by aggressive substances and efflorescence. These are influenced by environmental and construction factors, directly compromising system integrity [4-10].

Among the different types of staining, those caused by human action stand out, in which humans are the agents responsible for deterioration. Examples include graffiti and vandalism [11-12]. The

*Corresponding author.

eduardanovello@gmail.com (E. R. Novello); 0192073@feevale.br (K. L. D. Maus); 0331779@feevale.br (E. Gomes); projete@projeteengenharia.com.br (L. Lange); 0151420@feevale.br (R. M. Teles); alexandre.vargas@ufsm.br (A. S. de Vargas); daim@feevale.br (D. C. M. Arnold)

Received 14 January 2026; Revised 2 March 2026; Accepted 14 March 2026; Published online 18 August 2026

Copyright: © 2026 by the Author(s). Licensee Solarlits Limited (Hong Kong). This is an open access article distributed under the terms and conditions of the Creative Commons Attribution (CC BY) license.

Citation: Eduarda Rafaella Novello, Kim Lisbôa Daudt Maus, Eduardo Gomes, Leticia Lange, Ramon Mendonça Teles, Alexandre Silva de Vargas, Daiana Cristina Metz Arnold, Self-Cleaning Effect in Coating Mortar Promoted by the Addition of Zinc Oxide, Journal of Daylighting, 13:2 (2026) 451-462. doi: 10.15627/jd.2026.25

Table 1. Related studies.

References	Dye used	Concentration	Colorimetry Analysis
[3]	Methylene Blue	25 mg/L	Spectrophotometry (CIELab) and visual analysis
[27]	Rhodamine B	5 mg/L	Spectrophotometry (CIELab) and visual analysis
[21]	Methylene Blue	10 mg/L	Spectrophotometry (CIELab) and visual analysis
[20]	Rhodamine B	15 mg/L	Spectrophotometry (CIELab)
[28]	Methylene Blue	20 mg/L	Spectrophotometry (CIELab) and visual analysis
[18]	Rhodamine B and Methylene Blue	20 mg/L	UV photocatalytic reactor and color degradation measurement with a colorimeter
[22]	Rhodamine B and Methylene Blue	0,5 mg/L	Colorimetry (CIELab), visual analysis and image processing with ImageJ
[23]	Soot and Rhodamine B	0,5 mg/L	Spectrophotometry (CIELab)
[1]	Soot, ash and Rhodamine B	0,5 mg/L	Visual analysis from photographs, measurement by spectrophotometry (CIELab) and image processing with ImageJ

paints used in graffiti penetrate the pores of the mortar and hinder removal. According to [13], removal of such paints often requires aggressive chemical or mechanical methods such as strong solvents and high pressure washing, which can further damage the surface and leave persistent residual stains.

Studies such as [7,14-16,18-19], address research on the relevance of incorporating mineral additives with self-cleaning properties into surfaces. According to the authors, these materials are able to maintain their original visual characteristics even in aggressive environments due to the presence of photocatalytic compounds. During their study, [20] explain that this functionality is based on the ability of the surface to promote photocatalytic reactions activated by ultraviolet light (UV), degrading contaminants and microorganisms. Among the mineral additives studied, authors such as [21-23] highlight the use of zinc oxide (ZnO) as a photocatalyst because it is a metal oxide semiconductor and has strong capacity to degrade organic compounds, favored by high electron mobility, good photochemical performance and non-toxic nature.

According to [15,22,24], a reduction in peak load capacity is related to nanoparticle content exceeding the amount needed to react with available calcium hydroxide ($Ca(OH)_2$). Excess particles remain inactive and can lead to negative effects such as delayed cement hydration or silica leaching, which explains strength loss at higher contents. Studies such as [25], report that excessive ZnO incorporation can delay mortar curing time. Along with [26], they emphasize that zinc oxide has positive charge and can form new oxides and hydroxides. When exposed to high pH environments such as hydrated cement paste, insoluble zinc hydroxide ($Zn(OH)_2$) is formed. The presence of this semiconductor in cementitious matrices affects hydration kinetics and delays reactions, which can affect mechanical strength.

When comparing two mortar samples, a reference mortar and a mortar with added Zinc Oxide Hydroxyapatite powder (ZH), [18] used Rhodamine B and methylene blue dyes sprayed on the samples to evaluate degradation properties. All cement mortars were stained with and without ZH powder and then exposed in an enclosed chamber without external light under a UV lamp for 24 hours. The ZH modified mortar showed superior self-cleaning performance compared with plain cement mortar, assessed through a colorimeter.

Related studies presented in Table 1 support the current research and validate the methodology adopted for dye type, dye concentration and degradation analysis.

As such, this study aims to evaluate the incorporation of ZnO in coating mortars to assess the efficiency of methylene blue degradation in highly stained samples and the effects on pathological manifestations, improving aesthetics and durability.

2. EXPERIMENTAL PROGRAM

The study evaluates the physical, chemical, mechanical and self-cleaning changes resulting from the incorporation of different percentages (0, 1, 2, 3%) of ZnO into white cement-based mortar. The analytical grade ZnO used in the experimental program is a fine powder, amorphous and white, with pH 7 and purity of 99% according to the manufacturer's safety data sheet (SDS). To better understand the crystalline phases of zinc oxide and mortar, X ray diffraction (XRD) tests were performed using a Siemens Bruker AXS D 500 diffractometer with a copper tube (λ = 1.5406 Å) operating at 40 kV and 30 mA. A graphite monochromator and 1° and 0.01 mm slits were used. The samples were scanned from 5° to 80° (2θ) with a step of 0.02° per second. The specific surface area of the samples was obtained using the Brunauer Emmett Teller (BET) method. Pore volume and pore size distribution were evaluated using the Barrett Joyner Halenda (BJH) method. Both analyses were

Table 2. Nomenclature and quantity of materials per composition.

Composition	Dry material (g)	Water (g)	ZnO (g)	Percentages (%)
AZ-0	1250	405	0,00	0%
AZ-1	1250	405	12.50	1%
AZ-2	1250	405	25.00	2%
AZ-3	1250	405	37.50	3%

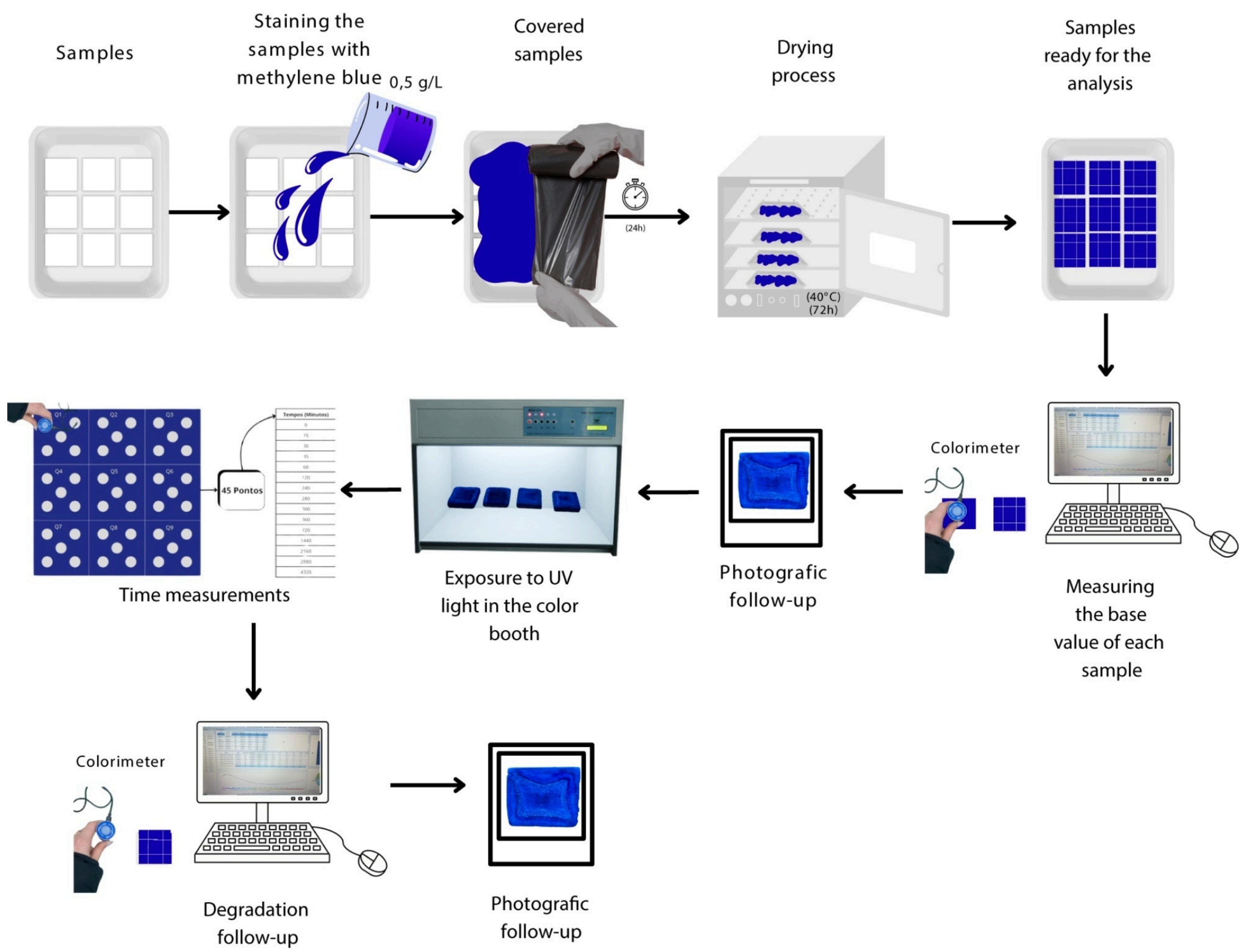

Fig. 1. Flowchart of method adopted during the self-cleaning performance analysis.

Table 3. Characteristics of methylene blue dye.

Physicochemical Properties	Specifications
Appearance	Solid, dark green
Molecular Weight	373.90 g/mol
Purity	97%

conducted with a Quantachrome NOVA Station A instrument, while the degassing was performed at 150°C for 20 hours.

The mortar used in the study is recommended for both internal and external coating.

Its composition includes Portland cement, dolomitic limestone, mineral fillers and additives, as pet the manufacturer's SDS. Mortar preparation followed NBR 16541 [29], with ZnO being added together with the dry components. An AG 5 mechanized mixer from Metal Cairo was used. The nomenclature and material quantities per molded mix are shown in Table 2. Before curing, all the compositions were evaluated by consistency index in triplicate, using the NBR 13276 [30] and bulk density followed the procedures established by NBR 13278 [31]. It is important to note that the water-to-binder ratio was fixed at 0,36, in order to observe the

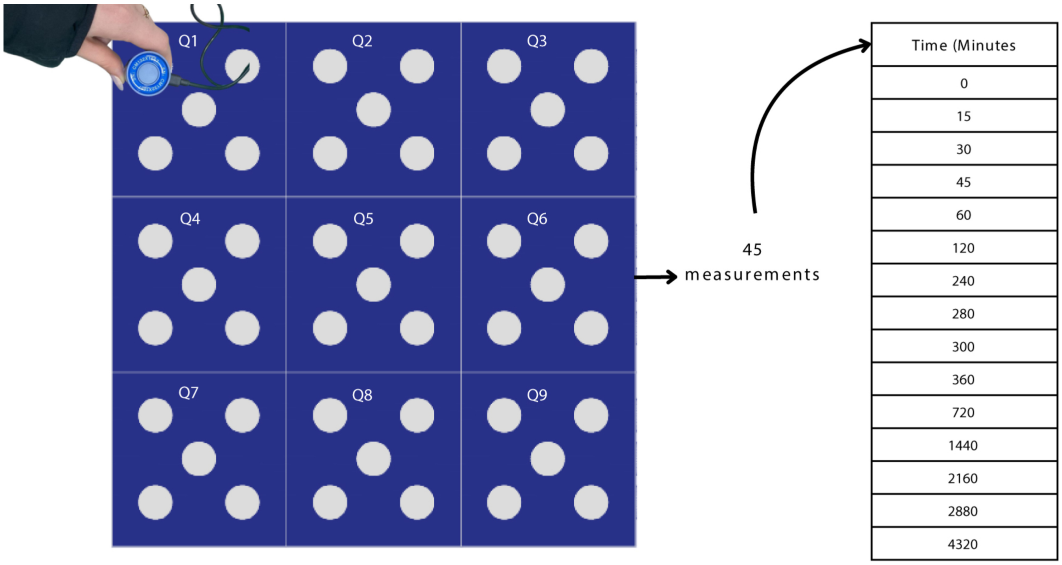

Fig. 2. Definition of quadrants, measurement points, and time intervals for conducting color variation measurements.

Table 4. Results of surface area, pore volume and pore radius tests for the ZnO and mortar samples.

Sample	Surface Area BET (m^2/g)	Surface Area BJH (m^2/g)	Pore volume (cc/g)	Pore radius (Å)
Mortar	6.09	2.801	0.005	15.729
ZnO	7.70	5.454	0.010	15.608

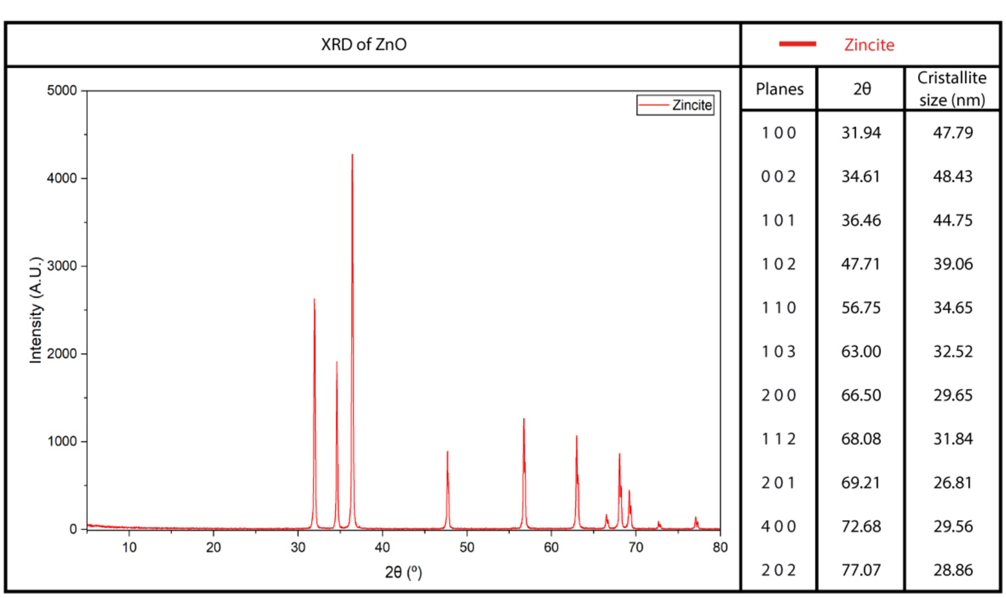

Fig. 3. X-ray diffraction of ZnO and crystal dimensions.

effect the zinc oxide would have in the workability of the mortar. In its hardened state, tests were conducted in triplicate, 28 days after casting using specimens measuring 4 cm ×4 cm ×16 cm. To analyze self-cleaning performance of the composition, three mortar plates measuring 8 cm × 7 cm × 2 cm were prepared for each of the compositions.

Bulk density tests in the hardened state followed NBR 13280 [32], capillary water absorption test times from NBR 15259 [33] were adapted to EN ISO 15148 [34] to classify the specimens according to NBR 13281-1 [35]. Flexural and compressive strength tests followed NBR 13279 [36] using an Instron Emic press, model DL2000. Self-cleaning performance was evaluated using the flowchart procedure depicted in Fig. 1.

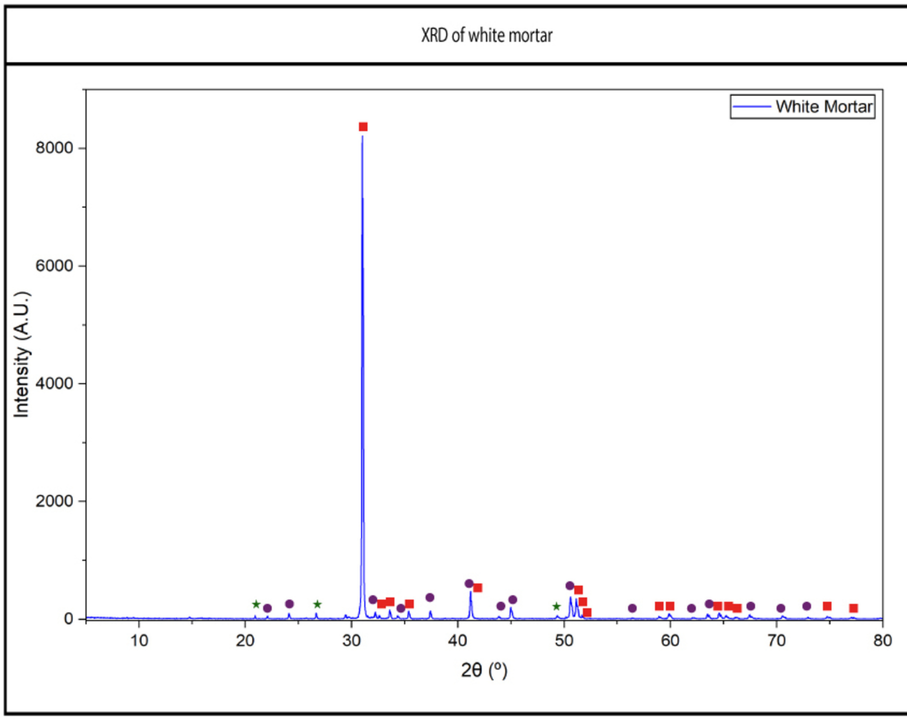

Hatutrite (Ca_3SiO_5)			Dolomite ($CaMg(CO_3)_2$)			Quartz (SiO_2)		
2θ	Planes	Cristallite size (nm)	2θ	Planes	Cristallite size (nm)	2θ	Planes	Cristallite size (nm)
31.03	0 1 5	56.98	22.12	0 1 2	91.46	20.95	0 0 6	87.25
32.62	0 1 8	123.54	24.15	1 0 4	61.22	26.70	0 0 9	78.43
33.62	1 1 3	44.05	32.25	1 0 7	123.43	49.36	3 0 0	34.03
35.4	0 2 4	52.02	34.36	2 0 2	53.24			
41.28	1 1 6	42.38	37.44	2 0 5	51.52			
51.15	1 0 1	38.9	41.2	1 2 2	42.37			
51.37	2 0 8	38.94	43.87	1 2 5	41.21			
51.69	1 1 0	38.99	44.99	1 0 1	39.79			
58.95	2 2 3	43.96	45.07	1 1 9	42.58			
59.9	3 0 6	31.36	50.62	1 2 8	38.78			
62.16	1 0 1	33.02	56.44	2 1 7	34.66			
64.6	1 1 2	38.72	63.5	1 1 1	32.14			
65.23	1 1 4	38.94	67.46	1 1 8	37.42			
66.16	2 1 4	39.13	70.57	1 2 1	29.09			
74.77	3 0 9	32.69	72.93	2 2 4	30.25			
77.03	2 2 6	28.15						

Fig. 4. X-ray diffraction of the mortar and crystal dimensions.

The mortar plates were submerged for 24 hours in an aqueous solution of methylene blue with 0.5% concentration. The goal was to stain the sample and simulate a pollutant. Table 3 shows the physicochemical properties of the methylene blue used, according to the manufacturer's SDS.

To evaluate photocatalytic activity, the mortar plates were exposed in a color assessment cabinet (BGD 276). The cabinet simulates solar radiation exposure and accelerates stain degradation through color and gloss loss, disintegration and oxidation.

Temperature remained constant at 25°C, while a pure UV lamp was used with 8,89 mW/cm² intensity, measured with the assistance of a radiometer. Figure 1 illustrates this procedure. After this step, the samples were exposed in a UV chamber at different time intervals for color variation measurements. According to EN 15886 [37], the surface analyzed must be representative of the material and the object as a whole. The number of measurement points must ensure statistically representative results. This study defined five measurement points in each quadrant of the sample, totaling 45 points per sample for the measurement times shown in Fig. 2.

Photocatalytic activity was assessed exclusively by means of surface colorimetry using a Color Density Meter Exact with 45/0 geometry. The light source was a balanced full spectrum LED. The wavelength range was 400 to 700 nm with 10 nm spacing. Measurement time was about 1.5 seconds.

The illuminant used was D65 with a 10 degree observer and the CIELab model. The colorimeter was used to assess and quantify color degradation over exposure time. The International Commission on Illumination (CIE) regulates technical report ISO/CIE 11664-5 [38], which defines the three-dimensional color space using nonlinear functions of the x, y and z coordinates. The L coordinate represents lightness on a scale from 0 to 100. Higher values indicate lighter shades and lower values indicate darker shades. The a* and b* parameters define chromaticity on the theoretical scale from −127 to +127. The a* axis expresses variations between green (negative values) and red (positive values). The b* axis expresses variations between blue (negative values) and yellow (positive values).

Based on these coordinates, the CIE recommended the use of an equation, composed of the L, a* and b* coordinates, to determine color differences between two measurement times on the same surface. Since color perception is subjective, the ΔE parameter became a way to convert color measurements into a numerical value that indicates perceptible differences according to visual perception categories. Different ΔE ranges correspond to different levels of perceptible color change. This study adopted the CIELab system and the ΔE parameter to quantify and evaluate color degradation variations of the samples in the different coordinates. This allowed the assessment of visual perceptibility associated with self-cleaning performance over 72 hours of exposure, in agreement with colorimetry evaluation methods reported in related studies (Table 1).

Table 5. Results of the characterization and classification of the mortars in the fresh state.

Composition	Consistency Index (mm)	Fresh State Bulk Density (kg/m³)	Classification NBR 13281-1(2023)
AZ-0	256	1796	1 800 ≤ DF < 2 000 (DE3)
AZ-1	235	1793	1 800 ≤ DF < 2 000 (DE3)
AZ-2	237	1799	1 800 ≤ DF < 2 000 (DE3)
AZ-3	242	1836	1 800 ≤ DF < 2 000 (DE3)

Table 6. Results of the characterization of the mortars in the hardened state.

Composition	Hardened State Bulk Density (kg/m³)	Classification NBR 13281-1 (2023)	Compressive Strength (MPa)	Flexural Tensile Strength (MPa)	Classification NBR 13281-1 (2023)
AZ-0	1522	1 400 ≤ DE < 1 600 (DE2)	3.1	1.3	0,5 ≤ Rf < 1,5(R2)
AZ-1	1204	1 200 ≤ DE < 1 400 (DE1)	3.5	1.8	1,5 ≤ Rf< 3,0 (R3)
AZ-2	1607	1 600 ≤ DE < 1 800 (DE3)	3.0	2.0	1,5 ≤ Rf< 3,0 (R3)
AZ-3	1198	DE < 1 200 (DE0)	3.2	2.2	1,5 ≤ Rf< 3,0 (R3)

3. RESULTS AND DISCUSSION

To evaluate the modifications in the mortar caused by ZnO incorporation on its mechanical and self-cleaning properties, the study first analyzed the crystalline structure and composition of the materials. From BET and BJH analyses, it was possible to determine the specific surface area, as well as the pore area, volume and radius of the pores of the ZnO samples and of the mortar, presented in Table 4. Results show that ZnO has a specific surface area 26.44% greater than the composite materials of the mortar. Therefore, there are good prospects for using ZnO in photocatalysis, since larger surface areas provide greater contact between the semiconductor and the molecules to be degraded, increasing the sites where chemical reactions can occur. A larger volume of smaller diameter pores was observed for ZnO compared with the mortar, which contributes to the previously discussed surface area, as also reported by [17,39,40].

To complement the previous analyses, chemical characterization of ZnO and the mortar was performed. Figure 3 shows the X ray diffraction (XRD) pattern of ZnO. The diffractogram displays diffraction peaks matched to card no. 00-210-7059 in the Crystallography Open Database (COD). This result confirms that the material consists of 100% zincite phase of ZnO, exhibiting a hexagonal wurtzite type structure, characteristic of ZnO nanocrystals. Studies by [41-44] present diffractograms with peaks equivalent to those observed in this study, supporting the analysis. Among the main phases of zinc oxide, the hexagonal wurtzite phase is the thermodynamically stable crystal form under ambient pressure and temperature, as explained by [45]. This semiconductor has a direct band gap of approximately 3.37 eV, a value that renders it highly active under ultraviolet radiation, a finding also reported by the same authors. Based on these explanations, ZnO is expected to favor the photocatalytic process and thus contribute to the self-cleaning properties in this study. Crystallite dimensions range from 26.81 to 47.79 nm, matching values reported by [46-48], who observed average sizes between 25 and 50 nm, characteristic of ZnO with hexagonal wurtzite structure. Through chemical analysis and surface area data, ZnO shows good potential as a photocatalytic agent, consistent with results reported by [18,22,49].

The mortar was also analyzed for chemical composition. Figure 4 presents the main diffraction peaks of the white mortar. The composition is represented by 94.3% dolomite ($CaMg(CO_3)_2$), with peaks identified by COD 00-120-0014, corresponding to dolomitic lime present in the material. Quartz (SiO_2) peaks account for 0.4% of the composition, shown by COD 00-901-0146, and are related to the mineral fillers of the mortar represented by the fine aggregate used in the mix. The remaining 5.3% detected in the diffractogram correspond to Hatutrite (Ca_3SiO_5), with main peaks indexed through COD 00-900-8366, a phase representative of Portland cement in the mixture. However, the average crystallite size of the mortar components is approximately 50 nm, values close to those found for ZnO.

To characterize mortars with different ZnO contents, Table 5 presents the results for the behavior of fresh state samples. Analysis of Table 5 shows that as the percentage of ZnO increases, the consistency index decreases compared with AZ-0, affecting mortar workability. This reduction in workability may be linked to the larger specific surface area and higher porosity of ZnO (Table 4), requiring more water to adequately lubricate the mix for flow on the consistency table. Similar results were observed by [50], who reported a 5.33% reduction in the consistency index when incorporating 0.3% ZnO. [51] reported reductions of 2.15% and 3.44% for 1% and 3% ZnO relative to the reference mix. Both [25,52] reafirm these behaviors, attributing the reduction in consistency index to increased viscosity and changes in particle interactions caused by ZnO addition. Reviewing bulk density results in the fresh state shown in Table 5, the mortars did not present expressive variations with ZnO addition at different percentages,

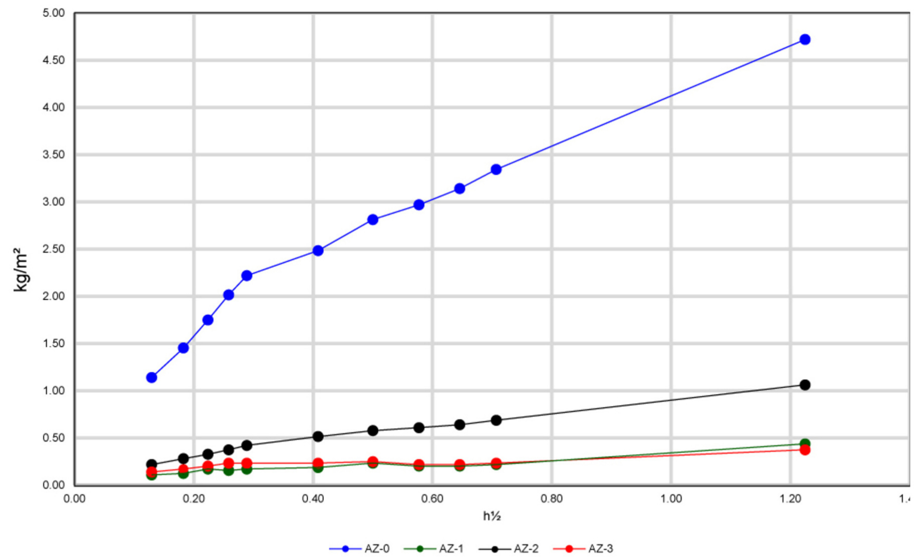

Sample	Time($h^{1/2}$)	Δ Absorption(kg/m^2)	Percentage relative to AZ-0 (%)	Class NBR 13281-1 (ABNT, 2023)
AZ-0	0.13	1.1	--------	4.0≤Wh<5.5 (W4)
	1.33	4.7		
AZ-1	0.13	0.1	90.73%	Wh<1.0 (W7)
	1.33	0.4		
AZ-2	0.13	0.2	77.48%	1.0 ≤Wh<2.5 (W6)
	1.33	1.1		
AZ-3	0.13	0.1	92.05%	Wh<1.0 (W7)
	1.33	0.4		

Fig. 5. Capillary water absorption coefficient.

remaining within the same normative classification range according to NBR 13281-1 [35].

To complement mortar characterization results, **Table 6** shows the outcomes of tests on mortars in the hardened state. Analyzing hardened bulk densities and classifying them according to NBR 13281-2 [53], ZnO incorporation resulted in different bulk density classes among the samples. The highest classes were assigned to mixes AZ-1 and AZ-2. Although ZnO incorporation produced variations in fresh state bulk density results, the change was not significant, with similar values. Compressive strength remained comparable after ZnO incorporation, with modifications in results but values similar to the reference mix AZ-0.

However, several studies show that ZnO incorporation influences hydration processes and therefore the mechanical performance of mortars. At low contents ZnO tends to improve compressive strength, as observed in AZ-1, due to better particle packing at early ages [24,54,55]. Conversely, higher ZnO doses cause retardation of hydration reactions due to formation of an amorphous zinc hydroxide layer $Zn(OH)_2$ over C_3S and C_2S phases, temporarily inhibiting hydration. With continued curing this layer transforms into calcium hydroxyzincate [$CaZn2(OH)_6 \cdot 2H_2O$], allowing reactions to resume and promoting late strength gain [25,27,56]. Thus, lower ZnO contents favor mechanical performance, while higher concentrations tend to partially reduce these properties. Still, in this study values obtained for ZnO modified samples remain close to the reference sample AZ-0, indicating the semiconductor does not strongly affect the material's mechanical properties.

Flexural tensile strength at 28 days showed behavior similar to that observed by [42], who with 0, 1, 2, 3, 4 and 5% ZnO in mortars with 1:3 mix ratio and w/c 0.5, found that increased ZnO content promoted gradual increase in flexural tensile strength. Gradual increases in flexural tensile strength for 1%, 3% and 5% ZnO with gains of 50%, 62% and 58%, respectively, where obtained by [24].

In the present study, incorporation of 3% ZnO by mass resulted in a 40.90% gain in flexural tensile strength relative to AZ-0. Samples were classified according to NBR 13281-1 [35], with AZ-0, AZ-1 and AZ-2 classified as R^2, while AZ-3 was classified as R3, associated with higher exhibited strength. Samples showed gradual behavior as ZnO content increased.

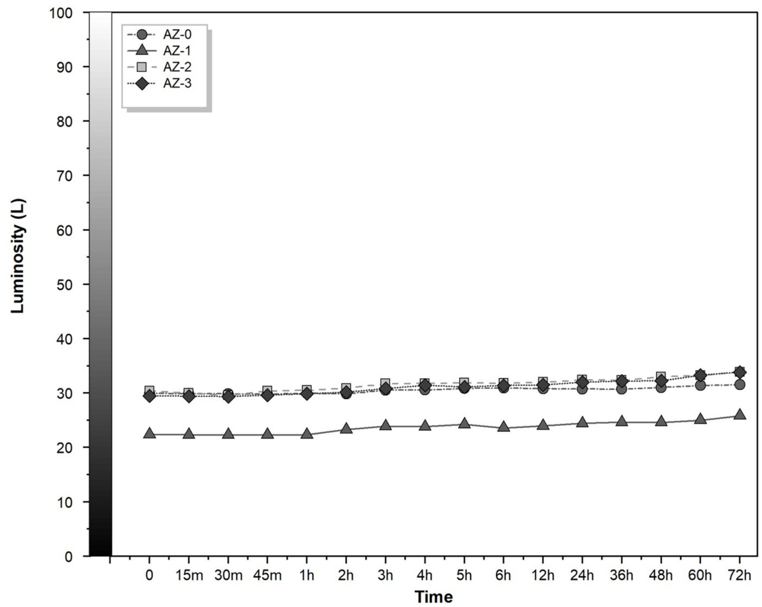

Fig. 6. Mortar luminosity (L) analysis.

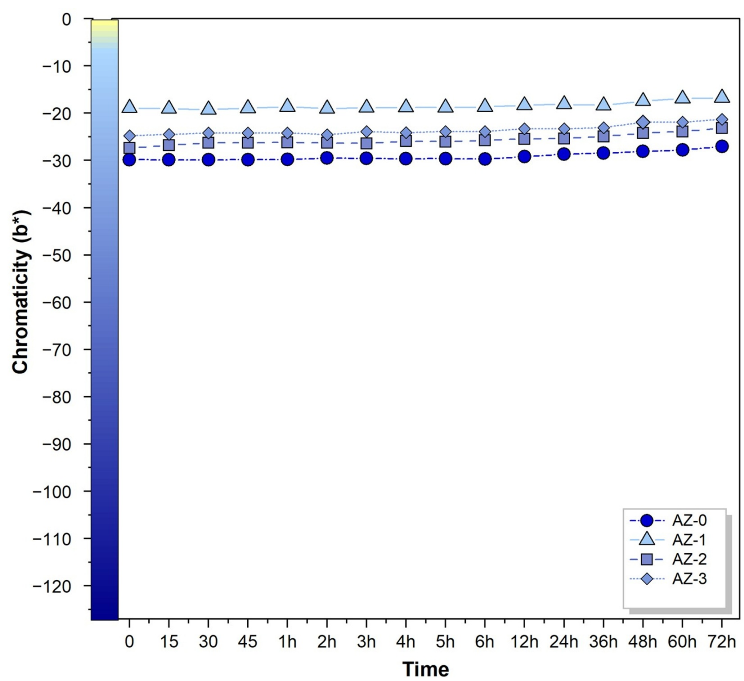

Fig. 7. Chromaticity analysis along the blue-yellow axis (b*).

Figure 5 shows that samples with ZnO incorporation presented lower capillarity coefficient values compared with AZ-0. According to Table 4, ZnO resulted in greater volume of smaller pores, larger surface area and thus better particle packing, yielding less porous mortars with lower surface capillary absorption. The graph observed in Fig. 5 shows that capillary absorption of AZ-1, AZ-2, AZ-3 is respectively 90.72%, 77.48% and 92.05% lower than AZ-0. This behavior is associated with higher surface porosity observed in AZ-0, which may result in greater capacity to absorb dirt when applied as facade render. ZnO incorporation promoted reduction in capillary absorption, indicating nanoparticles act to seal surface pores, a behavior not so evident in hardened bulk density and compressive strength tests. AZ-2 exhibits a reduction in capillary absorption comparable to the other zinc oxide mixtures, although with lower efficiency. This behavior is attributed to differences in ZnO dispersion within the cement matrix. The absorption pattern indicates a higher concentration of ZnO in the inner region of the specimen and a lower concentration near the surface.

As a result, fewer surface capillary pores are sealed, which leads to slightly higher water absorption compared to the other

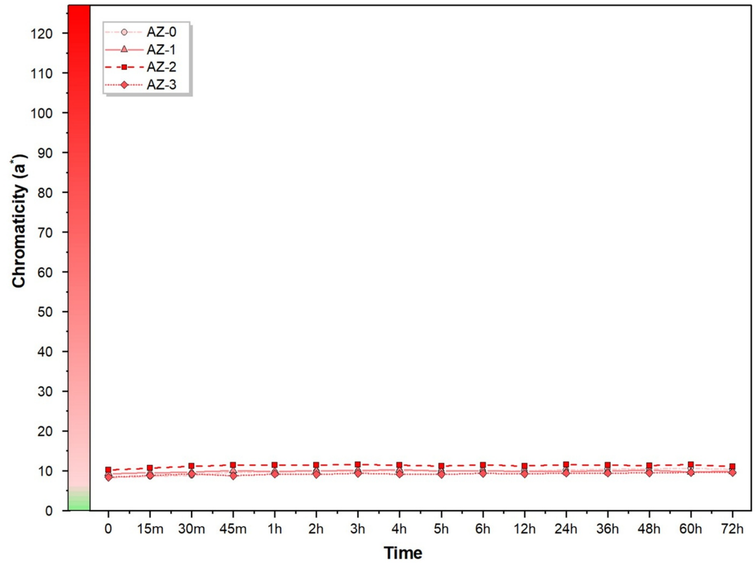

Fig. 8. Chromaticity analysis along the green-red axis (a*).

compositions. These results demonstrate ZnO contributes to reduced water absorption, sealing pore structure, limiting water penetration, mitigating moisture retention and consequently reducing pollutant adherence on mortar surfaces, thus contributing to samples' self-cleaning effect.

To evaluate self-cleaning performance and quantify color degradation over exposure time, color coordinate variations were assessed using the CIELab system. Figure 6 presents variations obtained for the L* coordinate, corresponding to lightness. Lightness L is expressed on a scale from black (0) to white (100), so higher values along the vertical axis indicate surface lightening. Figure 6 shows sample AZ-0, without ZnO, lightened by 5.29% comparing initial and final exposure times. Mixes with ZnO showed lightening of 15.5%, 11.45% and 14.78% for AZ-1, AZ-2 and AZ-3 respectively after 72 h exposure. Thus samples with ZnO showed greater lightening, demonstrated by degradation of methylene blue used here to simulate pollutants, confirming the photocatalytic effect. Sample AZ-1 showed the greatest lightening, despite small variations relative to the reference in fresh and hardened state characterizations. Superior lightening performance of AZ-1 may be associated with its higher density class and higher compressive strength. According to [1,27,57] reflectance and lightening increase when the surface becomes more compact and less rough.

To assess statistical significance of results, an ANOVA was performed (p-value = 2.67×10^{-25}; F = 118.83), which indicated significant differences among samples. Tukey test confirmed AZ-1 had mean luminosity values significantly lower than the others.

These results show ZnO incorporation directly influences mortar photocatalytic behavior, reinforcing the semiconductor's contribution to the material's self-cleaning effect. To confirm observed lightness degradation and corroborate [58] who reported similar trends, samples with ZnO showed higher L values, indicating increased lightening and confirming ZnO efficiency for photocatalysis.

The b* axis, representing blue-yellow variation in CIELab, was used to assess methylene blue degradation over exposure time as shown in Fig. 7. Negative b* values represent blue tones, in which numbers closer to -127 represent a richer tonality. Values closer to zero indicate loss of methylene blue coloration, evidencing self-cleaning. Figure 7 shows degradation of 9.37%, 11.41%, 15.46% and 14.07% for AZ-0, AZ-1, AZ-2 and AZ-3 respectively. Sample AZ-3 with 3% ZnO exhibited b* values closer to zero over time compared with AZ-0, indicating greater reduction of dye tonality and thus greater methylene blue degradation.

Although AZ-2 showed larger percentage degradation between final and initial times (Fig. 7), similar to the behavior observed in L, Tukey test confirmed AZ-1 presented the highest photocatalytic degradation index, differing significantly from the other samples and showing the highest average lightening over exposure time. AZ-0 maintained the lowest chromatic variation. Superior degradation performance of AZ-1 may be related to its better mechanical performance or to a smaller inicial value of b*, meaning that the degradation would be more apparent and therefore present as higher efficency. Comparing these results with [59], who reported that higher ZnO incorporation yields greater photodegradation efficiency, this study indicates higher photocatalytic efficiency at low concentrations, suggesting better semiconductor dispersion and larger active surface area without compromising mortar properties.

Chromaticity degradations of 9.37% (AZ-0), 11.41% (AZ-2), 15.46% (AZ-1) and 14.07% (AZ-3) were evaluated by ANOVA (p-value = $3,622,67\times10^{-35}$; F = 319.07), which showed statistically significant differences among compositions over exposure times.

https://dx.doi.org/10.15627/jd.2026.25

Table 7. Color classification parameters of the mortars.

Composition	Average measurement using the CIELAB system				Classification ISO/CIE11664-6 (2022)	Parameters (ΔE)
	L*	a*	b*	ΔE		
AZ-0 (T-0h)	30	8	-30	3.8	Clear Difference	3.5 – 5.0
AZ-0 (T-72h)	32	10	-27			
AZ-1 (T-0h)	22	9	-19	4.0	Clear Difference	3.5 – 5.0
AZ-1 (T-72h)	26	10	-17			
AZ-2 (T-0h)	30	10	-27	5.6	Large Difference	> 5.0
AZ-2 (T-72h)	34	11	-23			
AZ-3 (T-0h)	29	8	-25	5.7	Large Difference	> 5.0
AZ-3 (T-72h)	34	10	-21			

Studies such as [18,60,61] report trends different from this study, since those authors found greater photocatalytic efficiency with higher semiconductor incorporation in construction materials.

Another parameter assessed was chromaticity a*, shown in Fig. 8, representing green red variation. In this study a* did not show significant variation, as the dye used to simulate pollutants is blue. Therefore, color difference uses all coordinates (ΔE) previously mentioned. Despite different lightness and chromaticity variations, results obtained via Eq. (1), which expresses color classification parameters of the mortars (Table 7), show changes in values as ZnO content increases.

$$\Delta E = \sqrt{\Delta L^2 + \Delta a^{*2} + \Delta b^{*2}} \quad (1)$$

These indicate ZnO directly influences reflectance represented by L* and chromatic stability a* and b* of samples, linked to its photocatalytic efficiency. Results agree with [1,27,57] who observed significant ΔE changes in cementitious materials with higher percentages of various incorporated semiconductors.

Values in Table 7 are classified according to ISO/CIE 11664-5 [38], which defines visual perception ranges for color change, and as such is the method adopted in this study to evaluate which composition has the highest efficency. According to the bulletin, values greater than 3 indicate the color change is easily perceived by an observer. All evaluated samples presented ΔE above this threshold, showing the dye degradation over time was visually perceptible to the human eye, as also reported by [27]. In this study AZ-0 and AZ-1 recorded ΔE of 3.8 and 4.0 respectively, both classified as "noticeable difference", indicating a perceptible visual change but less intense than other samples. Samples with higher ZnO contents (AZ-2 and AZ-3) showed more expressive changes, with ΔE of 5.6 and 5.7, classified as "large difference". These results show observers perceive color alteration more intensely in those samples. This behavior is associated with combined variations in L, a* and b*, which represent lightness and chromaticities in CIELab. Among the coordinates, larger chromatic variations occurred along b* as shown in Fig. 7, consistent with use of methylene blue to simulate pollutants. The color degradation changes confirm that increased ZnO incorporation in mortars resulted in larger degradation ranges, evidencing the photocatalytic and self-cleaning effect over exposure time, and it is also noted that although the ΔE values show significant differences, a different staining method, such as spraying the dye and not submerging the sample in a dye solution, may result in even greater differences between compositions because the staining would be superficial and therefore easier to degrade.

4. CONCLUSION

The present study evaluated the influence of incorporating different contents of ZnO into a coating mortar on its chemical, mechanical and self-cleaning properties. XRD analyses confirmed that ZnO has a hexagonal wurtzite structure, yielding a specific surface area 26.44% greater than the dry mortar, which favors the samples' photocatalytic performance. An increase in ZnO content reduced mixture workability. However, fresh bulk density classes did not change. In hardened state tests, incorporation of 1% ZnO (AZ-1) produced the highest compressive strength, 3.5 MPa, 12.90% greater than AZ-0. This compressive strength change was not expressive for all ZnO mixes. Flexural tensile strength increased progressively with ZnO content, with AZ-3 showing the largest gain of 40.90% over AZ-0, reaching 2.2 MPa. Improved mechanical performance is associated with reduced porosity observed in the capillary water absorption test, with up to 92%

reduction in water percolation over time due to better particle packing and pore sealing.

Compositions exposed in a UV radiation chamber for 72 hours confirmed the photocatalytic and self-cleaning efficiency of ZnO modified mortars by colorimetric analyses in the CIELab system. The ΔE parameter supports the semiconductor's photocatalytic efficiency, since all samples showed color differences classified as perceptible to the human eye. AZ-2 and AZ-3 stood out for larger chromatic variations along the b* axis. Statistical analysis indicated significant differences in methylene blue degradation over time. Overall, results show that ZnO incorporation is a promising alternative for cementitious materials. At low contents it can enhance compressive strength. It reduces capillary water absorption and limits pollutant adherence on facades. Addition of this photocatalyst also improved the samples' self-cleaning performance, promoting degradation and reduction of pollutants simulated by methylene blue, thus helping preserve coating durability and appearance over time.

FUNDING

This work was supported by FAPERGS grant n° 81290.810.64533.08032024.

AUTHOR CONTRIBUTIONS

E. Novello – Conceptualization, Methodology, Investigation, Formal analysis, Writing – Original Draft

K. Maus – Methodology, Investigation, Writing – Review & Editing

E. Gomes – Investigation, Formal analysis

L. Lange – Investigation, Writing – Review & Editing

R. Teles – Methodology, Investigation, Writing – Review & Editing

A. Vargas – Investigation, Formal analysis

D. Arnold – Conceptualization, Methodology Writing – Review & Editing, Project Administration

DECLARATION OF COMPETING INTEREST

The authors declare no conflict of interest.

REFERENCES

[1] R. Casarin, et al. Ccomparação da eficiência da escovação na rápida mudança de cor em parede externa pela aplicação dedispersão de nano-tio₂ e de solução de naclo, in: Encontro Nacional de Tecnologia do Ambiente Construído - ENTAC, Canela, Brasil, 09-11 november 2022, pp 1-16.

[2] R. Terra, L, Levantamento de manifestações patológicas em revestimentos de fachadas das edificações da cidade de Pelotas, Programa de Pós-Graduação em Engenharia Civil, Universidade Federal do Rio Grande do Sul, Porto Alegre, 2001.

[3] G. Austria, Argamassa autolimpantes para revestimento de fachadas: o efeito das propriedades fotocatalíticas do dióxido de titânio, Programa de Pós-Graduação em Engenharia Civil, Universidade Federal do Rio Grande do Sul, Porto Alegre, 2015.

[4] M. Cincotto, M. Silva, H. Carasek, Argamassas de revestimento: características, propriedades e métodos de ensaio. São Paulo: Instituto de Pesquisas Tecnológicas. São Paulo, Brasil. 1995.

[5] R. Bauer. Patologia em revestimentos de argamassa inorgânica, in: Simpósio Brasileiro de Tecnologia das Argamassas - SBTA, Salvador, Brasil, 17-18 april 1997, pp 319-331.

[6] A. Masuero, Principais manifestações patológicas em revestimentos de argamassa. São Paulo: Escola Politécnica - USP, 2001.

[7] A. Silva, C. Fioriti, Mapeamento de manifestações patológicas em revestimentos argamassados externos de edifícios de múltiplos pavimentos, Revista Eletrônica de Engenharia Civil 15:2 (2020) 192-205.

[8] S. Santos, A. Laursen, Uma abordagem preliminar das manifestações patológicas mais comuns em construções residenciais, Revista Científica Multidisciplinar Núcleo do Conhecimento 12:11 (2022) 137-165.

[9] M. Santos, D. Schuch, Patologias em fachadas revestidas com argamassa estabilizada, in: XVII Congreso Latinoamericano de Patología de la Construcción, Santa Cruz de la Sierra, Bolivia, 28-30 september 2023.

[10] C. Branco, et al., Comparação de degradação de fachada com revestimento de argamassa no campus UFSM-CS, in: Encontro Nacional de Tecnologia do Ambiente Construído - ENTAC, Maceio, Brasil, 9-11 october 2022.

[11] D. Machado, Pensar sobre o vandalismo: os ataques contra o patrimônio cultural e as possibilidades de investigação no campo da história, in: Simpósio Nacional de História, Florianópolis, Brasil, 27-31 july 2015.

[12] F. Tavares, J. Wappler, Investigação das manifestações patológicas mais incidentes nas edificações escolares da rede municipal de Tubarão/sc, Curso de Engenharia Civil, Universidade do Sul de Santa Catarina, 2018.

[13] S. Amruktar, et al., Recent developments in the anti-grafitti coatings: an attentive review, Journal of coatings technology and research 13:3 (2022) 717-739.

[14] A. Fujishima, X. Zhang, Titanium dioxide photocatalysis: present situation and future approaches, Comptes rendus Chimie 9:5-6 (2006) 750-760.

[15] S. Raha, M. Ahmaruzzaman, ZnO nanostructures materials and their potential applications: progress, challenges and perspectives, Nanoscale Advances, 4:8 (2022) 1868-1925.

[16] J. Chen, C. Poon, Photocatalytic construction and building materials: from fundamentals to applications, Building and environment, 44:9 (2009) 1899-1906.

[17] P. Jedrejczak, et al., Physicomechanical and Antimicrobial Characteristics of Cement Composites with Selected Nano-Sized Oxides and Binary Oxide Systems. Materials, 15:2 (2022) 661. DOI: 10.3390/ma15020661.

[18] A. Mocioiu, et al., Self-cleaning and antibacterial properties of the cement mortar with zno/hydroxyapatite powders, Inorganics, 10:12 (2022) 241.

[19] H. Hu, et al., Experimental study on cement-based materials modified by nano-zinc oxide and nano-zirconia based on response surface optimization design. Materials, 18:7 (2025) 1515. DOI: 10.3390/ma18071515.

[20] F. Hamidi, F. Aslani, Tio_2-based photocatalytic cementitious composites: materials, properties, influential parameters, and assessment techniques. Nanomaterials, 9:10 (2019) 1444.

[21] C. Feltrin, Síntese e propriedades do zno: correlação entre propriedades estruturais e atividade fotocatalítica, Universidade Federal do Rio Grande do Sul, 2010.

[22] V. de Maria, et al., Advances in ZnO nanoparticles in building material: antimicrobial and photocatalytic applications-systematic literature review, Construction and Building Materials, 417 (2024) 135337.

[23] S. Pourali, et al., In situ synthesis of zno/g-c_3n_4 based composites for photodegradation of methylene blue under visible light. Scientific reports, 15 (2025) 462.

[24] D. Nivethitha, S. Dharmar, Efeito de nanopartículas de óxido de zinco na resistência da argamassa de cimento, International journal of science, technology & engineering, 3 (2016) 123-127.

[25] J. Liu, Q. Li, S. Xu, Influence of nanoparticles on fluidity and mechanical properties of cement mortar, Construction and building materials, 101 (2015) 892-901.

[26] G. Arliguie, J. Grandet, Étude de l'hydratation du ciment en présence de zinc : influence de la teneur en gypse. Cement and concrete research, 20:3 (1990) 346-354.

[27] J. Bersch, A. Masuero, D. dal Molin, Photocatalytic coloured rendering mortars: effect of tio_2 and iron oxide pigments on the physical, mechanical, hygric, and photoactive behaviour. Materials & structures, 56 (2023) 146.

[28] F. Maranhão, Método para redução de mancha nas vedações externas de edifícios. Escola Politécnica, Universidade de São Paulo, 2009.
[29] Associação Brasileira de Normas Técnicas, NBR 16541:2016, Argamassa para assentamento e revestimento de paredes e tetos - preparo da mistura para realização de ensaios. Rio de Janeiro, ABNT 2016.
[30] Associação Brasileira de Normas Técnicas, NBR13276:2016, Argamassa para assentamento e revestimento de paredes e tetos - determinação do índice de consistência. Rio de Janeiro: ABNT 2016.
[31] Associação Brasileira de Normas Técnicas, NBR 13278:2005. Argamassa para assentamento e revestimento de paredes e tetos - determinação da densidade de massa e do teor de ar incorporado. Rio de janeiro: ABNT, 2005.
[32] Associação Brasileira de Normas Técnicas, NBR 13280:2005. Argamassa para assentamento e revestimento de paredes e tetos - determinação da densidade de massa aparente no estado endurecido. Rio de janeiro: ABNT, 2005.
[33] Associação Brasileira de Normas Técnicas, NBR 15259:2005. Argamassa para assentamento e revestimento de paredes e tetos - determinação da absorção de água por capilaridade e do coeficiente de capilaridade. Rio de janeiro: ABNT, 2005.
[34] International Organization for Santardization. ISO 15148:2002 - Hygrothermal performance of building materials and products - Determination of water absorption coefficient by partial immersion. Geneva: ISO, 2002.
[35] Associação Brasileira de Normas Técnicas, NBR 13281-1:2023. Argamassas inorgânicas - requisitos e métodos de ensaios - parte 1: argamassas para revestimento de paredes e tetos. Rio de janeiro: ABNT, 2023.
[36] Associação Brasileira de Normas Técnicas, NBR 13279:2005. Argamassa para assentamento e revestimento de paredes e tetos - determinação da resistência à tração na flexão e à compressão. Rio de janeiro: ABNT, 2005.
[37] European Committee for Standardization. EN 15886:2010 - Conservation of cultural property - Test methods - Colour measurement of surfaces. Brussels: CEN, 2010.
[38] International Organization for Standardization. Iso/cie 11664-5:2024. Colorimetry - part 5: cie 1976 l*u*v* colour space and u', v' uniform chromaticity scale diagram. Geneva: ISO, 2024.
[39] V. Jašková, L. Hochmannová, J. Vytřasová, TiO2 and ZnO nanoparticles in photocatalytic and hygienic coatings. International journal of photoenergy, 1 (2013) 795060.
[40] H. Kamal, et al., Investigate the colloidal nano-zinc oxide addition on the strength acceleration of G-sand cement mortar, in: International Conference on Materials Engineering & Science, Baghdad, Iraq, 25-29 September 2019.
[41] M. Jabeen, et al., Chemical synthesis of zinc oxide nanorods for enhanced hydrogen gas sensing. Chinese physics b, 23:1 (2013) 018504.
[42] R. Gopalakrishnan, S. Nithiyanantham, Effect of ZnO nanoparticles on cement mortar for enhancing the physico-chemical, mechanical and related properties, Advanced science, engineering and medicine, 12:3 (2020) 348-355.
[43] M. Arefi, S. Rezaei-zarchi, Synthesis of zinc oxide nanoparticles and their effect on the compressive strength and setting time of self-compacted concrete paste as cementitious composites, International journal of molecular sciences, 13:4 (2012) 4340-4350.
[44] M. Lima, et al., Improving the mechanical properties of mortars by adding metal-doped zinc oxide nanoparticles, Engineering proceedings, 56:1 (2023) 331.
[45] A. Baig, M. Siddique, S. Panchal, A review of visible-light-active zinc oxide photocatalysts for environmental application, Catalysts, 15:2 (2025) 100.
[46] P. Mishra, M. Kantharia, Tensile strength investigation of cement mortar using nano zinc oxide (ZnO), Materials today: proceedings, 47 (2021) 7178-7180.
[47] S. Sahu, P. Samanta, Peak profile analysis of x-ray diffraction pattern of zinc oxide nanostructure, Journal of nano-and electronic physics, 13:5, 2021.
[48] M. Ramike, P. Ndungu, M. Mamo, Exploration of the different dimensions of wurtzite ZnO structure nanomaterials as gas sensors at room temperature, Nanomaterials, 13:20 (2023) 2810.
[49] B. Dehkordi, et al., A comparative study on the self-cleaning behavior and antibacterial activity of portland cement by addition of tio2 and zno nanoparticles, Materials research express, 8:3 (2021) 035403.
[50] P. Jędrzejczak, et al., Physicomechanical and antimicrobial characteristics of cement composites with selected nano-sized oxides and binary oxide systems, Materials, 15:2 (2022) 661.
[51] A. Augustyniak, et al., Investigating the release of zno nanoparticles from cement mortars on microbiological models. Applied nanoscience, 12:3 (2022) 489-502.
[52] S. Al-kasassbeh, et al,. Investigation of mechanical properties and microstructural development in cement-based materials incorporating zinc oxide nanoparticles, 2025.
[53] Associação Brasileira De Normas Técnicas. NBR 13281-2:2023: Argamassas Inorgânicas - Requisitos e métodos de ensaios - Parte 2: Argamassas para assentamento e argamassas para fixação de alvenaria. Rio de Janeiro, 2023.
[54] T. Nochaiya, et al., Microstructure, characterizations, functionality and compressive strength of cement-based materials using zinc oxide nanoparticles as an additive, Journal of alloys and compounds, 630 (2015) 1-9.
[55] M. Kantharia, P. Mishra, M. Trivedi, Strength of cement mortar using nano oxides: an experimental study, International Journal of Engineering and Advanced Technology, 8:3 (2019) 294-299.
[56] J. Tamashiro, et al., Doping engineering for controlled hydration and mechanical properties in portland cement mortar with ultra-low zno concentration, Journal of building engineering, 78 (2023) 107748.
[57] M. Diamanti, et al., Photocatalytic and self-cleaning activity of colored mortars containing Tio_2, Construction and building materials, 41 (2013) 167-174.
[58] X. Li, et al., Recent advances in noncontact external-field-assisted photocatalysis: from fundamentals to applications, ACS Catalysis, 11:8 (2021) 4739-4769.
[59] K. Chen, et al., Advancing photocatalytic concrete technologies for design, performance and sustainable futures, Advanced Nanocomposites, 1:1 (2024) 180-200.
[60] Q. Tang, et al., Preparation and Photocatalytic Performance of Nano-TiO2 Composite Decorative Panels Using the Multilayer Method, Iranian Journal of Science and Technology, Transactions of Civil Engineering, 49:1, (2025) 239-254.
[61] Y. Jasim, H. Kamal, M. Ali, Influence of Titanium Dioxide Nanoparticles on the Performance Characteristics of Cement-Based Mortar, Al-Rafidain Journal of Engineering Sciences, (2025) 141-146.

Disclaimer/Publisher's Note: The statements, opinions and data contained in all publications are solely those of the individual author(s) and contributor(s) and not of Solarlits and/or the editor(s). Solarlits and/or the editor(s) disclaim responsibility for any injury to people or property resulting from any ideas, methods, instructions or products referred to in the content.